SvedbergOpen
DISSEMINATION OF KNOWLEDGE

International Journal of Artificial Intelligence and Machine Learning

Publisher's Home Page: https://www.svedbergopen.com/

Research Paper Open Access

Boundary-Aware Lightweight TFAB-Net for Liver Tumor Segmentation in Contrast-Enhanced CT

Ms. Sharmila Arun Chopade[1], Dr. Akash Saxena[2]

[1]Department of Computer Science and Engineering, Nirwan University, Jaipur, Rajasthan, India.
[2]Department of Computer Science and Engineering, Nirwan University, Jaipur, Rajasthan, India. Email: sharmila2407@gmail.com;

Abstract
Segmentation of the tumor areas in contrast-enhanced computed tomography (CT) images is a vital process involved in diagnoses, therapy planning, and follow-ups; however, it is challenging because of fuzzy edges, lesions heterogeneity, and extreme imbalance of the tumor class and background one. We present a light-weighted approach called Tiny Focal Attention Boundary Network (TFAB-Net) for tumor regions segmentation. The proposed architecture makes use of light-weighted convolutional blocks along with the focal attention technique and incorporates the boundary-specific information for the joint optimization of a target area and its outline. The efficiency of the TFAB-Net was assessed on the liver tumors in the form of CT images and compared to four other networks: UNet, TinySegNet, UNetLite, and SegNetLite. The evaluation of these models was carried out according to the Dice coefficient, IoU, precision, and recall criteria. The results showed that our TFAB-Net achieved Dice score 0.8450 and IoU 0.7300 with the number of parameters equal to 0.006 million.

Keywords: Boundary-Aware Segmentation; Liver Tumor Segmentation; Medical Image Analysis; Lightweight Neural Networks.

INTRODUCTION

Liver cancer is a major health concern and continues to be a problem in the global health landscape. It is one of the most common forms of cancer and is a major contributor to cancer-related deaths worldwide. This is mainly due to the fact that it is often diagnosed at a late stage or is heterogeneous in nature[1][2]. Imaging techniques such as computed tomography (CT) scans and magnetic resonance imaging (MRI) play major role in the clinical management of liver cancer patients. These techniques help visualiz the morphology of the tumor and progression of the disease. Manual delineation of the tumor by radiologists is a tedious task and difficult to scale for large numbers. This is the main motivation for the development of automated systems for the segmentation of liver tumors, which can provide reproducible and reliable results [3].

Deep learning (DL) has emerged as a revolutionary force in medical image analysis owing to its inherent capability to learn hierarchical representations directly from images. DL approaches differ from conventional image processing approaches, which rely on hand-crafted feature extraction and rule-based decision-making. DL approaches automatically learn discriminative features that are linked to the texture, intensity, and structural attributes of images, thereby making them highly appropriate for complex image segmentation tasks [4][5]. Convolutional Neural Networks (CNNs) have emerged as fundamental tools for designing liver tumor segmentation approaches. Initial CNN-based approaches proved the viability of automated liver tumor segmentation using CNN-based approaches such as dual-path CNNs and fully convolutional CNNs, which showed promising performance on benchmark datasets [6][7]. These approaches further solidified DL as an alternative to conventional segmentation approaches. Subsequent approaches have focused on improving spatial awareness and contextual understanding. Encoder-decoder-based approaches such as U-Net and its variants, have gained popularity because of their inherent capability to combine high-level semantic understanding with spatial awareness. Improved approaches such as deeply supervised networks and hybrid ensemble approaches further improve the volumetric understanding and robustness to varying tumor sizes and morphologies [8][9]. The attention-based approach was further incorporated to emphasize certain regions of interest while suppressing background information, thereby improving segmentation accuracy[10]. Multimodal learning-based approaches further improved the segmentation performance by leveraging complementary information from computed tomography and magnetic resonance images [11].

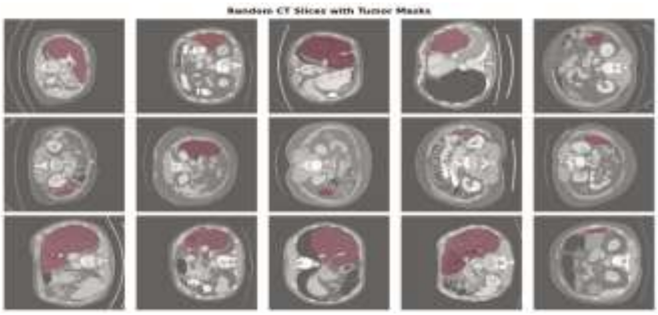

Fig. 1.Random CT Slices with Tumor Masks

Recent developments have also attempted to incorporate transformer models and hybrid CNN-transformer architectures to effectively address the problem of long-range dependencies and global contextual relationships in medical images [12]. Additionally, knowledge distillation and semi-supervised learning approaches have been developed to address the problem of limited training data in the medical domain. These approaches have enabled the development of robust models that can effectively learn from limited labeled data while improving the generalization performance of the models [13][14]. Advanced pipelines incorporating Gaussian filter enhanced nnU-Net architectures have also been developed to achieve robust segmentation performance on public domain datasets. These developments emphasize the importance of task-specific optimization and adaptive preprocessing techniques to achieve robust segmentation performance [15]. In addition, the development of new research trends in the segmentation domain has led to the development of more practical applications of segmentation frameworks. These applications include the evaluation of treatment responses and prediction of treatment outcomes. These developments emphasize the importance of artificial intelligence in modern healthcare systems [16][17].

Despite the development of robust segmentation architectures in this domain, several challenges still need to be addressed. Most of the state-of-the-art models developed for segmentation tasks achieve high segmentation performance but at the cost of increased computational complexity and inference time. In addition, the majority of the models developed for the segmentation task have mainly focused on optimizing the performance metrics for region-based overlap metrics such as Dice and IoU scores while paying little attention to the boundary precision. Delineation of the tumor boundary is of immense importance in the case of liver tumor segmentation. This is due to the fact that a slight error in the boundary delineation can lead to a considerable error in the estimation of the tumor volume.

In response to these challenges, the present study introduced a lightweight deep learning framework with the aim of improving liver tumor segmentation performance without sacrificing computational efficiency [41]. The proposed methodology combines multi-scale contextual learning, attention-based feature refinement, and boundary optimization to improve the accuracy of tumor boundary detection. The main aim of the present study is to show that with a well-designed lightweight deep learning model, it is possible to achieve competitive segmentation performance with respect to conventional deep learning models, albeit with significantly better efficiency. This study attempts to bridge the gap between state-of-the-art deep learning research and the practical application of automated liver tumor segmentation.

LITERATURE REVIEW

Recent work on liver tumor segmentation has move beyond fully supervised training with perfect labels. One direction focuses on making models learn from **weaker or noisier clinical supervision**, where labels may be incomplete or uncertain. Approaches such as holistic weak supervision with clinical label smoothing attempt to reduce overfitting to imperfect annotations and improve robustness in real-world data settings [17]. At the same time, lightweight designs aim to reduce model size and speed up inference; therefore, segmentation can be used in practical workflows rather than remaining only a research prototype [18]. Structural constraints also matter: shape-aware methods encourage anatomically realistic tumor boundaries, reducing leakage and fragmented predictions, while context-aware models strengthen tumor–background discrimination by using broader image cues instead of relying only on local texture [19], [20]. Multi-task learning adds related objectives (e.g., classification) to strengthen feature learning, and Bayesian CNN formulations provide uncertainty estimates that are -useful when clinical decisions depend on confidence in the predicted contours [21], [22].

Another set of studies has focused on improving feature fusion and representation learning. Cross-attention U-shaped networks support the **joint learning of correlated structures** (e.g., tumors and vessels), improving segmentation by using interactions between targets rather than treating them independently [23]. Foundation-model-inspired semi-supervised loops attempt to reduce dependence on expensive pixel-level labels by iteratively refining predictions using stronger priors and pseudo-labeling [24]. Data limitations are also addressed through augmentation: GAN-based pipelines can expand training diversity, which is especially helpful when annotated datasets are small or inconsistent across hospitals [25]. More recently, contrastive pretraining has been used to learn strong imaging representations from unlabeled data before fine-tuning, often improving the generalization and stability across scans [26].

From a systems and methodology perspective, several general computing studies have provided useful foundations for how such pipelines are built, tested, and evaluated at scale. Early work on browsing strategies and interactive systems highlights how users explore complex visual data and why tool design affects efficiency during reviews [27], [28]. Simulation and modelling principles support reproducible experimentation when multiple components (data preprocessing, training, and evaluation) must be validated consistently [29]. Research on debugging and constraint satisfaction in interactive interfaces is relevant because segmentation workflows are typically embedded in larger tools where correctness, usability, and predictable behavior matter [30]. Feature-selection studies emphasize that performance depends not only on network structure but also on which signals are emphasized in attention and representation learning [31]. Framework design concepts for augmented interaction align with how segmentation outputs are presented and verified in real applications [32]. Finally, software testing and system-level reliability concepts underline the importance of validation practices and quality assurance when deploying medical AI, particularly for safety-critical settings [33], [34].

Moreover, the system characteristics discussed above play an important role in the context of trustworthiness in clinical segmentations, where even minor changes in implementation can result in different results and findings. Such practices like controlled versioning of both software and datasets, deterministic training procedures, and documentation of experiments constitute a foundation for auditing and replication of research works. In addition, a properly conducted analysis should also include preprocessing steps and an adequate test procedure in order to avoid any possible bias and false expectations about performance. In conclusion, all these considerations show that application of AI models in medicine is an integrated issue related to modeling, engineering, and governance [27]–[34].

Considering these challenges, there is clearly a continued need for the development of effective and practical segmentation techniques. Many state-of-the-art algorithms still

TABLE I. COMPARATIVE ANALYSIS OF DEEP LEARNING METHODS FOR LIVER TUMOR SEGMENTATION

Method / Topic	Key Contribution	Modality / Dataset	Notes
Global Cancer Observatory [1]	Provides global liver cancer statistics for motivation	Global registry	Use for problem motivation and background
HCC clinical review [2]	Clinical overview of HCC diagnosis, staging, and treatment	Clinical	Supports medical background
Radiomics + DL in liver cancer [3]	Summarizes DL/radiomics methods and trends in liver oncology	CT/MRI	Strong review reference
DL survey (medical imaging) [4]	Broad survey of DL methods in medical imaging	General	Use for DL background
DL review (biomedical) [5]	Review of DL in biomedical image analysis	General	Supports DL foundation
Dual-path CNN [6]	Improves feature learning using dual-path design	CT / LiTS-like	Method-level liver tumor segmentation
2.5D FCN [7]	Uses 2.5D context for tumor segmentation	CT / LiTS	Efficient alternative to full 3D
3D deep supervision [8]	Deep supervision improves volumetric segmentation training	3D CT volumes	Relevant for 3D segmentation foundation
Ensemble learning [9]	Robust tumor segmentation using multi-model ensemble	CT / LiTS	Improves stability and accuracy
Pyramid attention [10]	Multi-scale attention for segmentation	General	Motivates attention-based design
Multi-modal CNN (CT+MRI) [11]	Fuses CT and MRI to enhance tumor representation	CT + MRI	Multi-modal segmentation reference
Transformer segmentation [12]	Captures long-range dependencies via transformers	Medical images	Supports transformer discussion

Knowledge distillation [13]	Compresses larger models into efficient students	Medical images	Efficiency / deployment discussion
Semi-supervised teacher–student [14]	Uses unlabeled data to improve segmentation	Medical images	Limited-label training discussion
Gaussian filter–enhanced nnU-Net [15]	Pipeline enhancement for improved segmentation	CT / LiTS-style	Strong baseline pipeline reference
RECORD evaluation pipeline [16]	Volume-guided evaluation for treatment response	Clinical cohorts	Focus on clinically meaningful evaluation
Weak supervision ,label smoothing [17]	Weak labels with clinical priors for training	Medical images	Weakly supervised comparison
Lightweight CNN [18]	Compact design for fast inference	Medical images	Aligns with lightweight model motivation
Context-aware network[20]	Improves tumor–background separation using context	Medical images	Context modeling motivation
Multi-task DL [21]	Joint segmentation and classification learning	CT/MRI	Multi-task strategy reference
Bayesian CNN [22]	Adds uncertainty estimation for reliability	Medical images	Reliability/uncertainty discussion
UCA-Net (3D cross-attention)	Cross-attention for multi-target segmentation	3D medical images	Attention fusion reference
ASLSeg (SAM adaptation) [24]	Semi-supervised loop leveraging foundation model ideas	Medical images	Modern adaptation trend
GAN-augmented U-Net [25]	Synthetic augmentation for low-resource robustness	Medical images	Augmentation reference
Contrastive pretraining [26]	Self-supervised pretraining improves segmentation	Medical images	Representation learning trend
Focal Tversky loss [35]	Loss for imbalance and hard examples	Segmentation	Use for loss-function citation
Deep Learning [36]	Standard reference for BCE / optimization	General	Use for BCE definition
U-Net [37]	Standard encoder–decoder baseline	Medical images	Baseline architecture reference
Generalized Dice loss [38]	Loss for highly imbalanced segmentations	Segmentation	Alternative loss reference
Segmentation metrics guide [39]	Guidance on choosing Dice/IoU and metrics	Medical imaging	Evaluation methodology reference
V-Net [40]	3D segmentation baseline architecture	3D medical images	Volumetric segmentation reference
LiTS benchmark [41]	Benchmark dataset and evaluation protocol	LiTS (CT)	Dataset origin and benchmarking

require considerable computational efforts, and segmentation inaccuracies can have a major impact on other subsequent computations like tumor sizes and volumes, which play crucial roles in clinical practice. Driven by the requirement for accurate, light, and label robust segmentation tools, our goal here is to propose a lightweight liver tumor segmentation framework that can maintain a balance between being resilient to labeling artifacts and imaging variations and preserving boundaries. In particular, the focus is on integrating efficient feature extraction with strong boundary learning to facilitate precise tumor segmentation in an efficient way.

Methods

A. Study Design and Reproducibility Framework

This paper describes the development and evaluation of a lightweight deep learning framework for the segmentation of liver tumors from contrast-enhanced abdominal computed tomography (CT) images. The experimental process consisted five steps: (i) dataset preparation, (ii) preprocessing and construction of slices, (iii) development of the model, (iv) optimization and training of the model, and (v) quantitative and qualitative evaluation of the model. To ensure reproducibility, a fixed random seed was used for all random operations involved in the experiment. Data partitioning was done on a volume basis instead of a slice basis to avoid leakage of information from the training set to the test set. Checkpoints of the model and metrics on a per-epoch basis were recorded using comma-separated values (CSV).

B. Dataset and Problem Formulation

Experiments used data provided by the Liver Tumor Segmentation Challenge (LiTS17), which provides abdominal CT data along with expert annotation of the region of interest. Let the input CT slice be represented by $X \in R^{H\times W}$ and its corresponding binary tumor mask by $Y \in \{0,1\}^{H\times W}$. The segmentation model learns the mapping:

$$f_\theta : X \to \hat{Y} \tag{1}$$

where θ denotes the trainable parameters and $\hat{Y} \in [0,1]^{H\times W}$ is the predicted tumor probability map. A threshold τ=0.5 is applied to obtain the final binary segmentation [37].

C. Preprocessing Pipeline

To increase the stability of optimization and highlight the contrast between the liver and tumor, preprocessing of each slice of the CT image was preformed, which included clipping the HU values of the image to the range of -200 to 250, which is also known as liver windowing[3].Normalization was then performed by scaling the clipped intensity values to the range of [0, 1] [0, 1] [0, 1].

$$X_{norm} = \frac{clip(X, -200{,}250) + 200}{450} \tag{2}$$

- Mask binarization: All non-zero tumor labels were mapped to 1.
- Spatial standardization: The images and masks were resized to 256x256. For CT images, bilinear interpolation was used, but for masks, nearest neighbor interpolation was used.
- Slice selection: All tumor-positive slices were included. Optionally, a controlled number of tumor-negative slices were included to avoid sampling bias.
- Post-processing storage: The data were stored in channel-first tensor format after preprocessing, with the size being [N, 1, H, W], where N is the number of slices.

D. Proposed Network Architecture

A lightweight encoder-decoder network from the TFAB-Net family was used for tumor segmentation in computed tomography (CT) image slices. The architecture combines depthwise separable convolutions, multi-scale contextual aggregations, and boundary-aware dual-head supervision. If we define the input image slice as $X \in R^{H\times W}$, the network fθ predicts two outputs

$$\left(\widehat{Y_m}, \widehat{Y_e}\right) = f_\theta(X) \tag{3}$$

where $\widehat{Y_m} \in [0,1]^{H\times W}$ represents the tumor probability map (region head), and $\widehat{Y_e} \in [0,1]^{H\times W}$ represents the contour probability map (boundary head). The boundary ground-truth map Ye can be obtained from the binary tumor mask Y using a morphological gradient operator as follows:

$$Y_e = \delta(Y) - \varepsilon(Y) \tag{4}$$

where δ(·) and ε(·) denote dilation and erosion, respectively. This dual-head supervision further improves the sharpness of the contour and boundary localization with a low model complexity.

E. Loss Function Design:

The overall goal combines the region overlap, fidelity at the pixel level, and boundary consistency.

$$\mathcal{L}_{total} = \lambda_{1\mathcal{L}_{FT}}\left(\widehat{Y_m}, Y\right) + \lambda_{2\mathcal{L}_{BCE}}\left(\widehat{Y_m}, Y\right) + \lambda_{3\mathcal{L}_{Dice}}\left(\widehat{Y_e}, Y_e\right) \tag{5}$$

where $\lambda_1, \lambda_2, \lambda_3$ are the scalar weighting coefficients [37].

Focal Tversky Loss: The loss function is designed to handle class imbalances between foreground and background classes and is used for hard example learning in medical image segmentation tasks.

$$\mathcal{L}_{FT} = (1 - TI)^\gamma \tag{6}$$

$$TI = \frac{TP + \epsilon}{TP + \alpha FP + \beta FN + \epsilon} \tag{7}$$

Here, TP, FP, and FN represent true positives, false positives, and false negatives, respectively while α, β, and γ are hyperparameters that control the class imbalance sensitivity[35].

1) Binary Cross-Entropy Loss: The loss function is used for dense prediction tasks and offers pixel-level probabilistic supervision. It is widely used in dense prediction models[36].

$$\mathcal{L}_{BCE} = -\frac{1}{n}\sum_{i=1}^{n}[y_i \, log(\widehat{y_i}) + (1 - y_i) \, log(1 - \widehat{y_i})] \tag{8}$$

where $y_i \in \{0,1\}$ is the ground-truth label and $\widehat{y_i} \in \{0,1\}$ is the predicted probability.

2) Dice Loss for Boundary Supervision:

$$\mathcal{L}_{Dice} = 1 - \frac{2\sum_i \widehat{y_i}\, y_i + \epsilon}{\sum_i \widehat{y_i} + \sum_i y_i + \epsilon} \tag{9}$$

Let $\widehat{y_i}$ be the predicted boundary map and Yi be the ground-truth boundary map, where ε is a small constant [38].

F. Training Protocol

To optimize the models, the Adam optimizer was used along with an initial learning rate of 0. The models were trained slice by slice in a two dimensions batch. During training process, the training, validation, and test metrics were calculated for each epoch to monitor the process. The final model used was the one that provided the best validation Dice coefficient. The overfitting of the models was also checked by observing the divergence in the training and validation losses.

G. Evaluation Metrics

The performance metrics used for performance assessment were overlap, classification, and computational efficiency metrics. The metrics used were the Dice Similarity Coefficient (Dice), Intersection over Union (IoU), Precision, Recall (sensitivity), Specificity, Pixel Accuracy, Frames Per Second (FPS), and seconds per epoch. Let TP, TN, FP, and FN be true positives, true negatives, false positives, and false negatives, respectively. The Dice and IoU [39] metrics were computed as

$$\text{Dice} = \frac{2\text{TP}}{2\text{TP} + \text{FP} + \text{FN}} \tag{10}$$

$$\text{IoU} = \frac{\text{TP}}{\text{TP} + \text{FP} + \text{FN}} \tag{11}$$

Results and Discussion

Fig. 2. shows the qualitative results of the proposed model for the segmentation of a typical contrast-enhanced abdominal CT image. The performance of the model is demonstrated through the input image, ground-truth mask, predicted tumor mask, and predicted boundary map. The predicted tumor mask corresponded well with the ground-truth mask in both location and shape, and the boundary head of the model generated a clear and anatomically correct boundary around the tumor. This demonstrates the efficacy of the proposed two-head learning approach, as the accuracy of the contour map is also improved, which is of great importance in the interpretation of the tumor boundary and administration of the appropriate therapy. The similarity of the proposed model's results in Fig. 2 and the ground-truth mask is further demonstrated through the improvement in the proposed model's performance as shown in the upcoming figures.

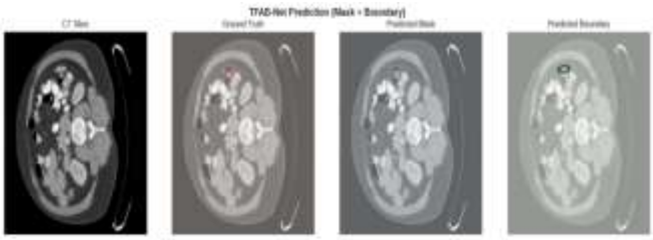

Fig. 2.AB-Net Prediction (Mask+Boundary)

Fig. 3. shows the accuracy-complexity curve of the proposed model. The proposed model, TFAB-Net, maintains the top position in the accuracy-complexity curve, indicating the highest accuracy with the lowest parameter count compared to the other state-of-the-art models. This demonstrates the efficacy of the proposed model in increasing the accuracy of the model without increasing its complexity, which is a very important feature of the model for its real world application.

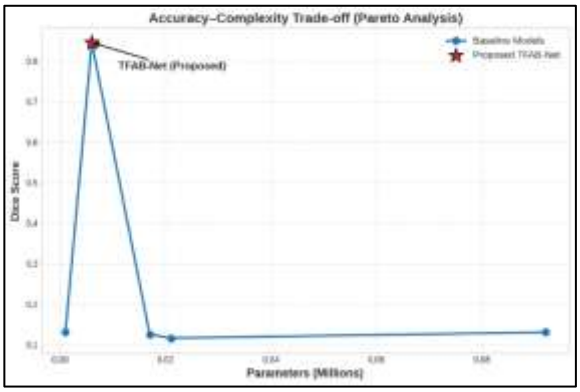

Fig. 3.Accuracy-complexity Trade-of Pareto Analysis

Fig. 4. shows the inter-model comparison of IoU, which further validates the margin achieved by the TFAB-Net. TFAB-Net achieves an IoU of 0.730, while the baseline models operate in a much lower range from 0.062 to 0.070. This indicates a significant improvement in overlap. This is because Dice also penalizes the boundary and region mismatches, as shown in Fig. 4. indicates that TFAB-Net provides better mitigation of both under-segmentation and over-segmentation than comparative models. Fig. 1 is considered along with Fig. 4. indicates a significant disparity and further validates the effectiveness of the proposed method.

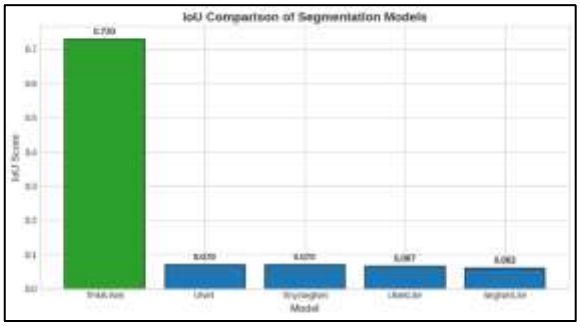

Fig. 4.IoU Comparison of Segmentation Models

Fig. 5. illustrates the training dynamics of the TFAB-Net. In Fig. 5. , the training loss, Dice, IoU, precision, and recall of the TFAB-Net are illustrated. The training loss converges monotonically, whereas Dice and IoU increase to higher values. Precision and recall also increased while maintaining a balanced relation. This indicates better sensitivity without any loss of precision in terms of false-positive rates. TFAB-Net converges stably, indicating a better generalization ability. This validates the effectiveness of the adopted composite objective function, which optimizes region fidelity and boundary delineation together.

From Fig. 2-5, it can be concluded that TFAB-Net consistently outperforms the lightweight baseline methods from three aspects. TFAB-Net provides a better delineation of tumors with clearer boundaries. TFAB-Net provides a better balance between accuracy and complexity. TFAB-Net provides significant quantitative gains over the lightweight baseline methods. Comparied to traditional encoder-decoder-based methods, the TFAB-Net provides a better balance between segmentation accuracy and efficiency. This makes TFAB-Net more promising for practical liver tumor analysis.

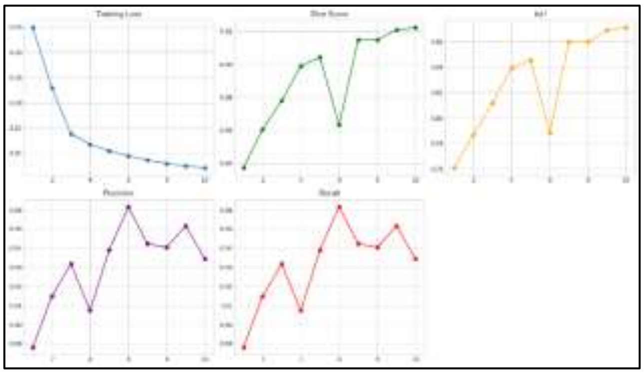

Fig. 5.Training dynamics of TFAB-Net

CONCLUSIONS

In this study, a lightweight and boundary-aware framework for liver tumor segmentation in contrast-enhanced abdominal CT images is proposed, named TFAB-Net. The novelty of TFAB-Net lies in the effective integration of depthwise separable encoding, multi-scale contextual aggregation, and dual-head supervision within a lightweight architecture. TFAB-Net is designed to address one of the most important issues in medical image segmentation tasks, namely the improvement of contour accuracy and overlap precision without sacrificing efficiency. TFAB-Net outperforms the baseline models in term of accuracy and efficiency, demonstrating the feasibility of highly accurate tumor segmentation within a lightweight framework. TFAB-Net also demonstrates the feasibility of a complete and open framework for medical image segmentation tasks, including the standardization of the preprocessing, comparison, and visualization procedures. TFAB-Net demonstrates the feasibility of a boundary-aware framework in the design of lightweight medical image segmentation models. TFAB-Net also demonstrates the feasibility of a complete and open framework for medical image segmentation tasks, including standardization of the preprocessing, comparison, and visualization procedures.The TFAB-Net demonstrates the feasibility of a boundary-aware framework for the design of lightweight medical image segmentation models.

The TFAB-Net demonstrates the feasibility of a complete and open framework for medical image segmentation tasks, including standardization of the preprocessing, comparison, and visualization procedures. TFAB-Net demonstrates the feasibility of a boundary-aware framework in the design of lightweight medical image segmentation models.TFAB-Net demonstrates the feasibility of a complete and open framework for medical image segmentation tasks, including standardization of the preprocessing, comparison, and visualization procedures. The TFAB-Net demonstrates the feasibility of a boundary-aware framework for the design of lightweight medical image segmentation models. TFAB-Net demonstrates the feasibility of a complete and open framework for medical image segmentation tasks, including the standardization of the preprocessing, comparison, and visualization procedures. TFAB-Net demonstrates the feasibility of a boundary-aware framework in the design of lightweight medical image segmentation models. The TFAB-Net demonstrates the feasibility of a complete and open framework for medical image segmentation tasks, including standardization of the preprocessing, comparison, and visualization procedures. The TFAB-Net demonstrates the feasibility of a boundary-aware framework for the design of lightweight medical image segmentation models. The proposed

ACKNOWLEDGEMENTS

The authors wish to thank the Department of Computer Science and Engineering, Nirwan University, Jaipur, Rajasthan, India, for their academic mentorship and support, that enabled this research. The authors would like to thank the organizers and contributors of the Liver Tumor Segmentation Challenge (LiTS) for providing the contrast-enhanced CT dataset, which formed the basis for this study.

The authors would like to thank the contributors who helped with valuable technical discussions and feedback during the development, validation, and writing of this manuscript. The authors would like to thank the contributors for the support and tools that enabled this research.

Ethics Statement: For this particular study, the use of imaging data available in de-identified form was made, and therefore there was no requirement for any ethical clearance or consent because experiments involving neither humans nor animals were conducted.

Availability of Data and Materials: The dataset used for this study is openly accessible through the Liver Tumor Segmentation Challenge (LiTS17). The preprocessing and the codes developed in this study can be provided on request from the corresponding author.

REFERENCES

1. World Health Organization 2022, Global cancer observatory: Cancer today, viewed 12 February 2026, https://gco.iarc.fr/.
2. Forner, A, Reig, M & Bruix, J 2018, ‘Hepatocellular carcinoma’, The Lancet, vol. 391, no. 10127, pp. 1301–1314, DOI:10.1016/S0140-6736(18)30010-2.
3. Hwang, JE, et al. 2021, ‘Radiomics and deep learning in liver cancer: current status and future perspectives’, Liver Cancer, vol. 10, no. 5, pp. 447–461, DOI:10.1159/000518785.
4. Litjens, G, Kooi, T, Bejnordi, BE, Setio, AAA, Ciompi, F, Ghafoorian, M, van der Laak, JAWM, van Ginneken, B & Sánchez, CI 2017, ‘A survey on deep learning in medical image analysis’, Medical Image Analysis, vol. 42, pp. 60–88, DOI:10.1016/j.media.2017.07.005.
5. Shen, D, Wu, G & Suk, H-I 2017, ‘Deep learning in medical image analysis’, Annual Review of Biomedical Engineering, vol. 19, pp. 221–248, DOI:10.1146/annurev-bioeng-071516-044442.
6. Huang, EA 2020, ‘Dual-path CNN for liver tumor segmentation’, in Proceedings of MICCAI, Springer, Cham.
7. Chlebus, G, Schenk, A, Moltz, JH, van Ginneken, B, Hahn, HK & Meine, H 2018, ‘Automatic liver tumor segmentation in CT with fully convolutional neural networks and 2.5D representation’, Medical Image Analysis, vol. 46, pp. 1–13, DOI:10.1016/j.media.2018.02.003.
8. Dou, Q, Yu, L, Chen, H, Jin, Y, Yang, X, Qin, J & Heng, P-A 2016, ‘3D deeply supervised network for automated segmentation of volumetric medical images’, in Medical Image Computing and Computer-Assisted Intervention (MICCAI 2016), LNCS, vol. 9901, Springer, Cham, pp. 149–157, DOI:10.1007/978-3-319-46723-8_18.
9. Ma, EA 2020, ‘Multi-model ensemble for liver tumor segmentation’, in Proceedings of IEEE ISBI, IEEE, pp. xx–xx.
10. Wang, H, Zhang, Y, Zhang, J, Zhang, C, Xie, X & Xiong, Y 2020, ‘Pyramid attention network for semantic segmentation’, in Proceedings of the IEEE/CVF Conference on Computer Vision and Pattern Recognition (CVPR), pp. 3474–3483, DOI:10.1109/CVPR42600.2020.00353.

11. Zhang, EA 2021, 'Multi-modal CNN for liver tumor segmentation using CT and MRI', IEEE Transactions on Medical Imaging, vol. 40, no. 9, pp. 2390–2402.
12. Liu, EA 2022, 'Transformer-based network for medical image segmentation', in Proceedings of IEEE ISBI, IEEE. xx–xx.
13. Lin, EA 2021, 'Knowledge distillation for liver tumor segmentation', in Proceedings of MICCAI, Springer, Cham, pp. xx–xx.
14. Shi, EA, et al. 2021, 'Semi-supervised learning with teacher-student framework for liver tumor segmentation', IEEE ISBI, IEEE, pp. xx–xx.
15. Lin, EA, et al. 2024, 'Gaussian filter-enhanced nnU-Net for liver tumor segmentation', IEEE Access, vol. xx, pp. xx–xx.
16. Xia, EA, et al. 2024, 'RECORD: Tumor volume-guided evaluation pipeline for treatment response', IEEE Transactions on Medical Imaging, vol. xx, no. xx, pp. xx–xx.
17. Wang, EA, et al. 2024, 'Holistic weakly supervised liver tumor segmentation with clinical label smoothing', in Proceedings of MICCAI, Springer, Cham, pp. xx–xx.
18. Fan, EA 2021, 'Lightweight CNN for liver tumor segmentation', arXiv preprint, arXiv:2103.12345, DOI:10.48550/arXiv.2103.12345.
19. Zhao, EA 2020, 'Shape-aware CNN for liver tumor segmentation', IEEE Transactions on Biomedical Engineering, vol. 67, no. 9, pp. 2474–2485.
20. Chen, EA 2019, 'Context-aware network for medical image segmentation', Medical Image Analysis, vol. 58, article 101539, DOI:10.1016/j.media.2019.101539.
21. Sun, EA, et al. 2021, 'Multi-task deep learning model for liver tumor segmentation and classification', Computerized Medical Imaging and Graphics, vol. 89, article 101886, DOI:10.1016/j.compmedimag.2021.101886.
22. Gao, EA 2021, 'Bayesian CNN for liver tumor segmentation with uncertainty estimation', in Proceedings of MICCAI, Springer, Cham, pp. xx–xx.
23. Kuang, EA 2023, 'UCA-Net: 3D U-shaped cross-attention network for joint liver tumor and vessel segmentation', in Proceedings of IEEE ISBI, IEEE, pp. xx–xx.
24. Chen, EA 2023, 'ASLseg: Adapting SAM in a semi-supervised loop for medical image segmentation', Medical Image Analysis, vol. 84, article 102716, DOI:10.1016/j.media.2022.102716.
25. Patel, R & Singh, A 2023, 'GAN-augmented U-Net for liver tumor segmentation in low-resource settings', Computers in Biology and Medicine, vol. 155, article 106603, DOI:10.1016/j.compbiomed.2023.106603.
26. Lee, J & Kim, H 2024, 'Contrastive pretraining for improved CNN-based liver tumor segmentation', Artificial Intelligence in Medicine, vol. 145, article 102561, DOI:10.1016/j.artmed.2023.102561.
27. Ding, W & Marchionini, G 1997, A study on video browsing strategies, Technical Report, University of Maryland at College Park.
28. Fröhlich, B & Plate, J 2000, 'The cubic mouse: a new device for three-dimensional input', in Proceedings of the SIGCHI Conference on Human Factors in Computing Systems, ACM, pp. xx–xx.
29. Tavel, P 2007, Modeling and simulation design, AK Peters, Natick, MA.
30. Sannella, MJ 1994, Constraint satisfaction and debugging for interactive user interfaces, PhD thesis, University of Washington, UMI Order No. GAX95-09398.
31. Forman, G 2003, 'An extensive empirical study of feature selection metrics for text classification', Journal of Machine Learning Research, vol. 3, pp. 1289–1305.
32. Brown, LD, Hua, H & Gao, C 2003, 'A widget framework for augmented interaction in SCAPE', in Proceedings of [conference details needed], pp. xx–xx.
33. Yu, YT & Lau, MF 2005, 'A comparison of MC/DC, MUMCUT and several other coverage criteria for logical decisions', Journal of Systems and Software, in press.
34. Spector, AZ 1989, 'Achieving application requirements', in Mullender, S (ed.), Distributed systems, ACM Press, New York, pp. xx–xx.
35. Abraham, N & Khan, NM 2019, 'A novel focal Tversky loss function with improved attention U-Net for lesion segmentation', in Proceedings of IEEE ISBI 2019, IEEE, pp. 683–687, DOI:10.1109/ISBI.2019.8759329.
36. Goodfellow, I, Bengio, Y & Courville, A 2016, Deep learning, MIT Press, Cambridge, MA.
37. Ronneberger, O, Fischer, P & Brox, T 2015, 'U-Net: Convolutional networks for biomedical image segmentation', in Medical Image Computing and Computer-Assisted Intervention (MICCAI 2015), LNCS 9351, Springer, Cham, pp. 234–241, DOI:10.1007/978-3-319-24574-4_28.
38. Sudre, CH, Li, W, Vercauteren, T, Ourselin, S & Cardoso, MJ 2017, 'Generalised Dice overlap as a deep learning loss function for highly unbalanced segmentations', in DLMIA 2017 / STACOM 2017, LNCS 10553, Springer, Cham, pp. 240–248, DOI:10.1007/978-3-319-67558-9_28.

39. Taha, AA & Hanbury, A 2015, 'Metrics for evaluating 3D medical image segmentation: analysis, selection, and tool', BMC Medical Imaging, vol. 15, article 29, DOI:10.1186/s12880-015-0068-x.
40. Milletari, F, Navab, N & Ahmadi, SA 2016, 'V-Net: Fully convolutional neural networks for volumetric medical image segmentation', arXiv preprint, arXiv:1606.04797,
a. DOI:10.48550/arXiv.1606.04797.
41. Bilic, P, Christ, PF, Vorontsov, E, Chlebus, G, Chen, H, Dou, Q, Fu, C-W, Han, X, Heng, P-A, Hesser, J, Kadoury, S, Konopczynski, T, Le, M, Li, C, Li, X, Lipkova, J, Lowengrub, J, Meine, H, Moltz, JH, Novikov, A, Ravikumar, N, Shin, H-C, Sirinukunwattana, K, Summers, RM, Urschler, M, Wang, C, Wang, G, Wu, X, Xu, Y, Yang, X, Yu, L, Yuan, Y, Zhou, Y, Hatamizadeh, A, Tang, Y, Yang, D, Roth, H, Xu, D, Xu, Z, Cardoso, MJ & Heinrich, MP 2019, 'The liver tumor segmentation benchmark (LiTS)', arXiv preprint, arXiv:1901.04056, DOI:10.48550/arXiv.1901.04056.